Translational Oncology 23 (2022) 101472

Contents lists available at ScienceDirect

Translational Oncology

journal homepage: www.elsevier.com/locate/tranon

Original Research

Correlation of changes in subclonal architecture with progression in the MMRF CoMMpass study

Gurvinder Kaur [a,1], Lingaraja Jena [a,1], Ritu Gupta [a,*], Akanksha Farswan [b], Anubha Gupta [b,*], K Sriram [c]

[a] Laboratory Oncology Unit, Dr. B. R.A. IRCH, AIIMS, New Delhi
[b] SBILab, Department of Electronics and Communication Engineering, IIIT, Delhi
[c] Department of Computational Biology & Centre for Computational Biology, IIIT, Delhi

ARTICLE INFO

Keywords:
Multiple myeloma
Clonal evolution
Actionable genes
Oncogenic correlations
Gene enrichment pathways
Molecular signatures

ABSTRACT

Multiple myeloma (MM) is a heterogeneous plasma cell proliferative disorder that arises from its premalignant precursor stages through a complex cascade of interactions between clonal mutations and co-evolving microenvironment. The temporo-spatial evolutionary trajectories of MM are established early during myelomatogenesis in precursor stages and retained in MM. Such molecular events impact subsequent disease progression and clinical outcomes. Identification of clonal sweeps of actionable gene targets in MM could reveal potential vulnerabilities that may exist in early stages and thus potentiate prognostication and customization of early therapeutic interventions. We have evaluated clonal evolution at multiple time points in 76 MM patients enrolled in the MMRF CoMMpass **study**. The major findings of this study are (a) MM progresses predominantly through branching evolution, (b) there is a heterogeneous spectrum of mutational landscapes that include unique actionable gene targets at diagnosis compared to progression, (c) unique clonal gains/ losses of mutant driver genes can be identified in patients with different cytogenetic aberrations, (d) there is a significant correlation between co-occurring oncogenic mutations/ co-occurring subclones e.g., with mutated TP53+SYNE1, NRAS+MAGI3, and anticorrelative dependencies between FAT3+FCGBP gene pairs. Such co-trajectories may synchronize molecular events of drug response, myelomatogenesis and warrant future studies to explore their potential for early prognostication and development of risk stratified personalized therapies in MM.

Introduction

Multiple myeloma (MM) is a plasma cell malignancy characterized by a complex genomic landscape, heterogeneity in response to therapy and clinical outcomes [1]. Myelomatogenesis is a multistep process that is initiated and driven by accumulation of composite genomic aberrations [2–7]. The primary cytogenetic aberrations include translocations involving IgH locus (found in about 55% patients) and hyperdiploid trisomies of odd numbered chromosomes (found in about 40% patients) [8,9]. While IgH translocations t(4;14) (partner *FGFR3*), t(14;16) (*MAF*) and t(14;20) (*MAFB*) have been associated with high risk disease and poor prognosis; other translocations t(11;14) (*CCND1*), t(6;14) (*CCND3*) and trisomies are considered to be associated with standard risk [10]. Deletion 13q is also considered to be an early event and is observed in about 35% of the patients. There are additional multiple secondary events that evolve gradually and include mutations in RAS/NFkB pathway genes, haploinsufficiency of p73, high expression of *MYC*, 1q gain, 1p loss and others. Recently, 8 copy number subtypes [11] and 12 RNA subgroups [12] of MM, have also been characterized from the Multiple Myeloma Research Foundation (MMRF) CoMMpass study [13].

Molecular analysis of myeloma genome through conventional cytogenetics and fluorescence in situ hybridization (FISH), gene expression profiling, Whole Genome Sequencing (WGS), Whole Exome Sequencing (WES) and microarrays has provided novel insights into the genomics of MM [14–17], role of driver genes [18–22] and chromothripsis [23,24], in risk prediction strategies and identified different oncogenic events involved in the immunity-malignancy equilibrium in MM [25,26]. Multiple mechanisms involving deregulated signaling cascades can derail oncogenic pathways [27,28] and their evaluation can lead to development of pathway directed therapies [29] for MM.

* Corresponding authors.
E-mail addresses: drritu.laboncology@aiims.edu (R. Gupta), anubha@iiitd.ac.in (A. Gupta).
[1] Both Gurvinder Kaur and Lingaraja Jena contributed equally.

https://doi.org/10.1016/j.tranon.2022.101472
Received 11 September 2021; Received in revised form 3 June 2022; Accepted 20 June 2022

A series of studies have established clonal heterogeneity in MM [30–33]. There is evidence that as disease progresses from its premalignant stages of MGUS (Monoclonal Gammopathy of Undetermined Significance) and SMM (Smouldering MM) to MM [34], the (sub)clones tend to evolve new mutations and CNAs (copy number alterations), imposed by positive selection pressure, and sweep to dominance [35–39]. It has been reported that the genomic landscapes of SMM are very similar to those at MM with two major patterns of progression [35]. While the static progression model retains the subclonal architecture as disease progresses to MM, a spontaneous evolution model supports changes in subclonal composition. A recent study [37] evaluated both Darwinian positive selection and neutrality in evolution in WGS CoMMpass data and surmised that neutral mutations might occur in a few tumors but Darwinian evolution appears to be the overall dominant trajectory of MM.

The temporal and spatial clonal trajectories established by the time of SMM are thus preserved and can predict the course of subsequent tumor evolution and contribute to drug resistance [35–37]. This also provides a unique opportunity to revisit and deploy prognostication at premalignant stages and adopt early intervention. There is limited information available on subclonal evolution associated with progression in MM and, in particular, on clinically relevant actionable targets. Moreover, there is no report on associations between co-occurring clonal gains/ losses in MM. This enthused us to evaluate clonal landscapes of the MMRF CoMMpass WES data at baseline time point (TP1) and compare to subsequent time points of progression (TP2, TP3, TP4 and TP5). We have analyzed 76 MM patients for whom multiple time point WES data were available in the MMRF IA12 dataset, and compared clonal mutational landscapes and pathways, at baseline with those at progression.

This study has shown that clonal expansion to progression in MM follows predominantly branching pattern of evolution, with differential waxing and waning of mutated (sub)clones. A series of subclonal mutations in driver and actionable genes could be identified, some of which showed patterns of mutational/ subclonal co-occurrence or exclusions with significant correlations. Identification of serial correlative clonal trajectories of drivers and actionable targets in MM may advance prognostication and assist in personalization of targeted therapies particularly at early stages of myelomatogenesis.

Materials and methods

A complete workflow of data analysis starting from selection of MMRF CoMMpass IA12 dataset to generation of FISH plots showing patterns of clonal evolution and interpretations is summarized in Fig. 1.

Selection of dataset

In this study, we have used the WES data obtained from the MMRF CoMMpass database (IA12) (https://themmrf.org/finding-a-cure/our-work/the-mmrf-commpass-study/), which includes whole genome/ exome sequencing data of over 1000 newly diagnosed MM patients with

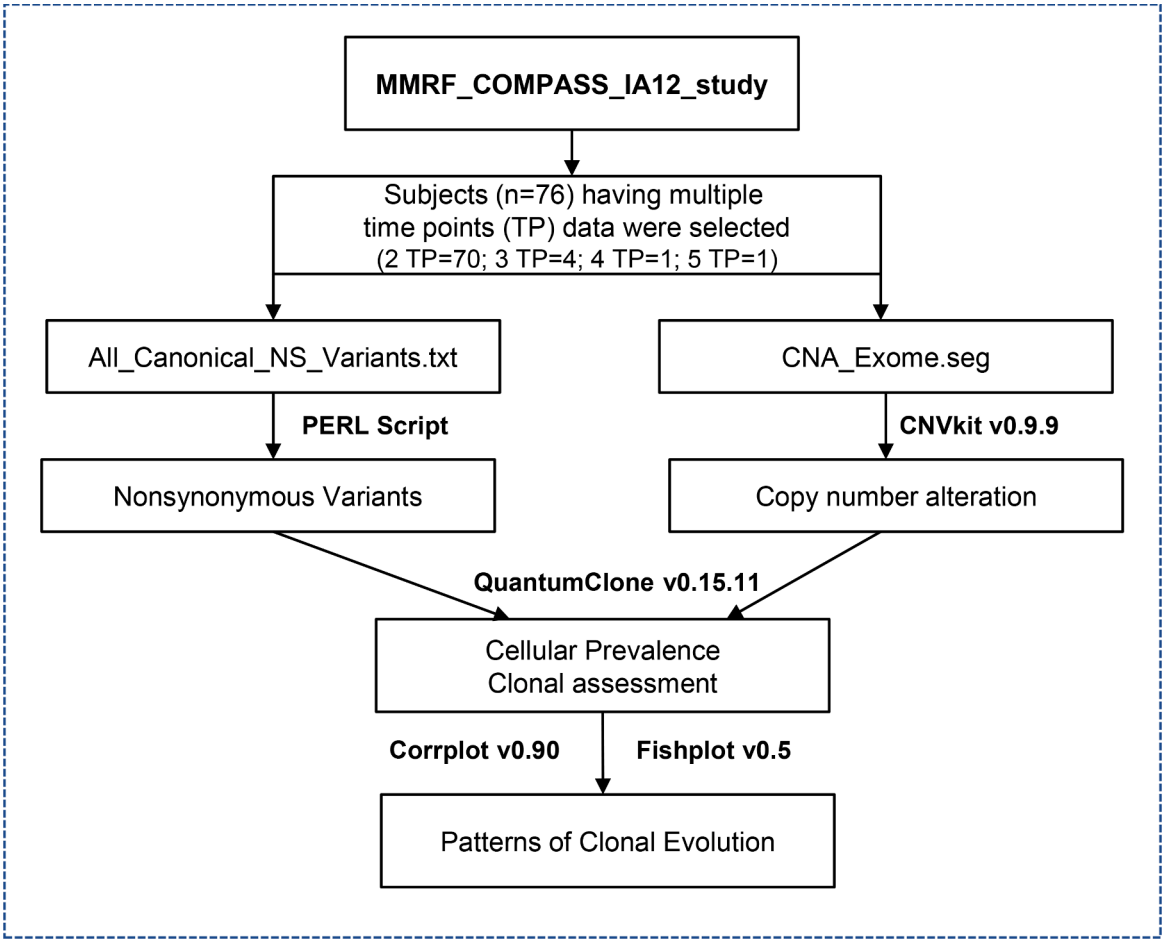

Fig. 1. Overall study design and workflow. Data on WES was mined for 76 MM patients sampled at multiple time points TP (ranging between 2 and 5) in the MMRF CoMMpass study IA12. Nonsynonymous mutations and copy number alterations were collated with PERL and CNVkit respectively. Data was converted into cellular prevalence with QuantumClone and analyzed further for mutation clustering and clonal assignments. Fishplot was used to deduce patterns of clonal evolution while corrplot was used to compare pairwise correlations among clonal shifts.

enriched tumor and matched constitutional samples. The variant file (MMRF_CoMMpass_IA12a_All_Canonical_NS_Variants.txt) and the copy number file (MMRF_CoMMpass_IA12a_CNA_Exome.seg) were used for this clonal evolution study. Clinical and demographic details were obtained from the Clinical_Flat_Files and are summarized in Table 1. The MM subjects ($n = 76$) having multiple time points data on Non Synonymous (NS) variants and CNAs (at 2 time points, $n = 70$; at 3 time points, $n = 4$; at 4 time points, $n = 1$; at 5 time points, $n = 1$) were selected and included in this study.

Evaluation of multiple time point whole exome data for cellular prevalence

We developed in house PERL (practical extraction and report language) scripts to parse single nucleotide variant / copy number variant (CNV) files for selected subjects at all timepoints. The CNVkit program (version 0.9.9; https://github.com/etal/cnvkit [40]) was used to extract absolute copy number from the copy number segment files (MMRF_CoMMpass_IA12a_CNA_Exome.seg). The output obtained from the CNVkit program was used to assign genotype information for each variant. The data obtained was further processed with QuantumClone [41] (https://www.rdocumentation.org/packages/QuantumClone/versions/0.15.11). Somatic variants along with their genotype information were used to infer the clonal progression in MM. The cellular prevalence values $\theta^{'}$ of each cluster were calculated as follows:

$$\widehat{\theta} = VAF \times \frac{N_{Ch} + N_{Ch(Normal)} \times \frac{1-p}{p}}{NC}$$

Table 1
Clinical, laboratory parameters and cytogenetic aberrations found in 76 MM patients.

Parameter	No. of patients	%
Median Age (Range) In Years	67 (35 to 93)	
Gender		
Male	43	56.6
Female	33	43.4
Hemoglobin (g/dL)		
≤10	76	100
>10	0	0
Platelet Count (/dL)		
<100	3	3.9
≥100	73	96.0
Serum creatinine (mg/dL)		
≤2	66	86.8
>2	10	13.2
Serum albumin (g/dL)		
<3.5	31	40.8
≥3.5	44	57.9
NA	1	1.3
ISS 1/2/3/NA	22/26/26/2	
RISS I/II/III/NA	8/38/6/24	
Serum calcium, mg/dL		
0–11	76	100
>11	0	0
IgG Isotype		
IgA	9	11.8
IgG	18	23.6
NA	49	64.5
BM plasma cells,%		
≤40	48	63.2
>40	6	7.9
NA	22	28.9
Serum LDH (IU/L)		
≤420	47	61.8
>420	13	17.1
NA	16	21.1
β2-microglobulin, mg/L		
<3.5	29	38.2
≥3.5	45	59.2
NA	2	2.6

NA = Not available.

where N_{Ch} is the number of copies of the corresponding locus in cancer cells, $N_{Ch(Normal)}$ is the number of copies of the corresponding locus in the normal cells ($N_{Ch(Normal)} = 2$ for autosomes), VAF is the Variant Allele Frequency and *NC* is the number of chromosomal copies bearing the variant and *p* is the tumor purity [41].

Assessment of patterns of clonal evolution

The values of cellular prevalence obtained from QuantumClone were subjected to Fish plot R package [42] in order to visualize the patterns of clonal evolution (https://github.com/chrisamiller/fishplot). Cellular prevalence values higher than 1 were set to 1 as suggested [41]. Clonal lineage was inferred by following sum rules and cross rules as described in earlier studies [43,44]. Patterns of evolution [45] were classified as branching if characterized both by the gain and loss of mutational clusters at relapse or as linear if characterized by the gain of mutations at relapse but no evidence of clonal loss. Stable evolution pattern was characterized by a preserved clonal structure at both the time points. Stable with loss patterns had a predominantly preserved clonal structure at relapse but with some loss of cluster of mutations.

Estimation of clonality and subclonality

Based on the value of estimated cellular prevalence percentage, gene variants were classified into four categories: Clonal (C, cellular prevalence > = 85%), High Sub Clonal (HSC, cellular prevalence > = 25% and < 85%), Low Sub Clonal (LSC cellular prevalence > = 0.6% and <25%), Very Low Sub clonal (VLSC, cellular prevalence <0.6%)] [46].

Identification of mutated genes and gene functions

Genes found to be mutated were classified as drivers/ oncogenes/ tumor suppressor/actionable genes as defined by intOgen [47] (https://www.intogen.org/search); OncoKB [48] (https://www.oncokb.org/); cBioPortal [49,50] (https://www.cbioportal.org/) and COSMIC actionability data v93 (https://cancer.sanger.ac.uk/cosmic).

Computation of pairwise correlations between subclones

Pearson correlation between pairwise subclonal mutations was evaluated and visualized with corrplot function of the corrplot package v0.90 (https://cran.r-project.org/web/packages/corrplot/index.html).

Analysis of biological pathways

The Kyoto Encyclopedia of Genes and Genomes (KEGG) pathways relating to mutations at TP1 and TP2 (time point 2) were deduced by gene enrichment approach using Enrichr (https://maayanlab.cloud/Enrichr/) as described [51] while MSigDB [52] was used to compare molecular signatures at both timepoints respectively.

Results

NS mutational spectrum at baseline compared to progression

A median of 60 NS mutations (range 2 to 414) and 65 NS variations (range 2 to 312) were identified per patient at baseline and on progression respectively. Supplementary Table ST1 lists 915, 1173 and 2444 genes that were found to have NS mutations in whole exomes of samples evaluated at TP1 or TP at progression (TP2) or in common at both the time points respectively.

Among these, 16 genes (ALK, ATR, AXL, BIRC3, BRIP1, CSF3R, DDR1, MERTK, MET, PTPN11, RAD52, RICTOR, RPTOR, TET2, U2AF1, XRCC3) and 14 genes (BLM, ETV6, FANCM, FLT4, JAK2, KMT2A, PIK3R1, POLE, RAD51C, RFC1, RFC2, SLX4, SMO, TSC1) were

actionable genes and were identified only at baseline or on progression respectively. A group of 32 actionable genes (APC, ASXL1, ATM, ATRX, BRAF, CBFB, CCND1, DAXX, DDR2, ERBB3, ERBB4, ERCC3, FGFR3, FGFR4, GNAQ, KIT, KRAS, MLH1, MLH3, MTOR, MYC, NRAS, NTRK2, NTRK3, PML, POLD1, PRKDC, RB1, SF3B1, SMARCA4, TEK, TP53) were found to be mutated at both the time points (Supplementary Table ST1).

Gains and losses of mutated genes in subclones with progression

A comparison of clonal gains or losses of mutated genes from baseline to progression in patients is shown in Supplementary Table ST2. The most commonly mutated actionable genes included NRAS followed by *KRAS, TP53, BRAF, GNAQ, NTRK3, APC, RB1* and *FGFR3* in descending order while mutations were also common in other genes such as *TTN, RRBP1, FAT3, DNAH5, MUC16, DIS3, USH2A* and *IRF4* (Supplementary Table ST2).

The genes that showed topmost number of clonal gains or losses with progression in MM patients are shown in Fig. 2a. The topmost frequent clonal gains were observed in *NRAS, RRBP1, TP53, FCGBP, SYNE1, KCNMA1, BRAF* and *MAGI3* while the most frequent clonal losses on progression were found among *ZFHX3, LAMA1, MASP1* and *PTPRF* (Fig. 2a). All these mutated genes were observed at comparable high subclonal levels except *RRBP1* that was found at low subclonal levels at both the time points (Fig. 2b). Heatmaps in Fig. 3 and Supplementary Fig. 1 depict frequencies of clonal losses or gains of mutated actionable and non actionable genes in each of the 76 MM patients respectively as well as their cytogenetic profiles.

Comparison of cellular prevalence of mutated genes at baseline with progression

Average%CP of mutated genes at baseline (TP1) and second TP of progression (TP2) were calculated with QuantumClone and are plotted in Fig. 4. Some of the genes that were clonal (average%CP > = 85%) at diagnosis dropped down to low subclonal levels (*LOXHD1*%CP = 24.871), or high subclonal levels (*ICOSLG*%CP = 28.972, *VCAN*%CP =

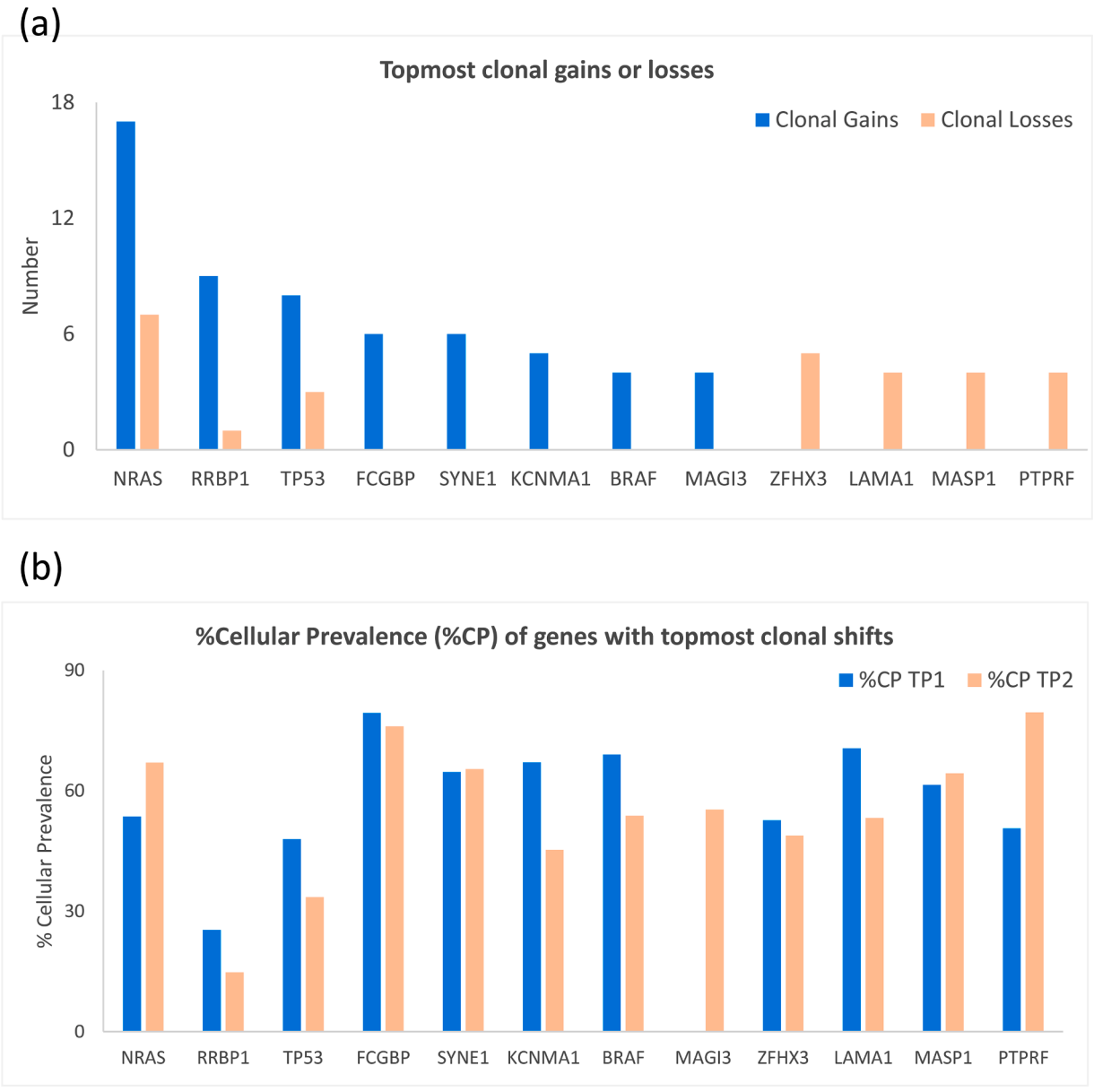

Fig. 2. Comparison of topmost clonal gains and losses associated with progression of MM. (a) Genes showing largest numbers of clonal gains and losses, and (b) parallel comparison of cellular prevalence of genes shown in (a).

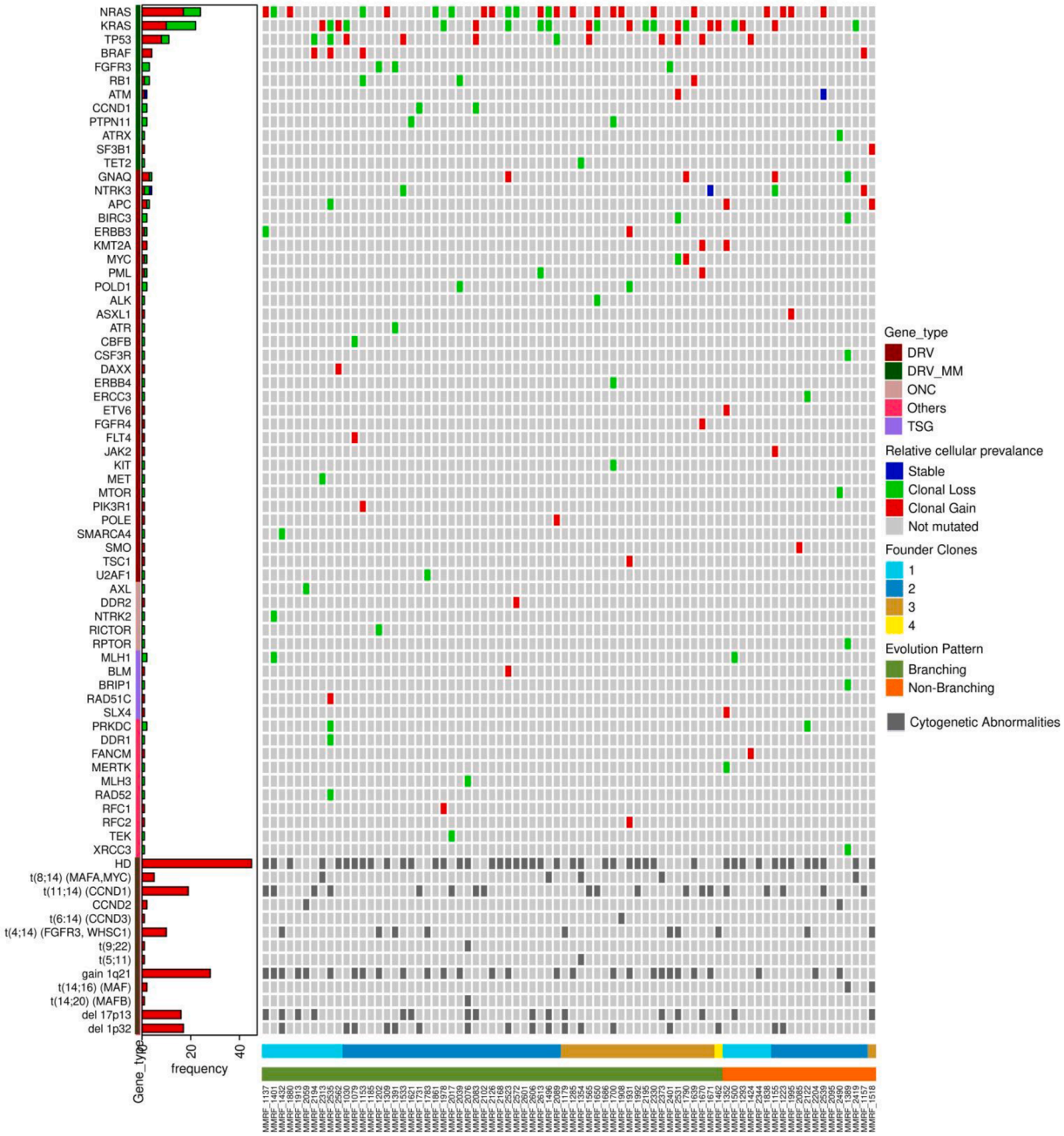

Fig. 3. Heatmap depicting distribution of clonal shifts in actionable genes and cytogenetic aberrations in 76 MM patients categorised on the basis of branching/ non branching evolution and number of founder clones. DRV = Driver, DRV_MM = Driver known for MM, ONC = Oncogene, TSG = Tumor suppressor gene.

47.3278, *DST*%CP = 41.394, *RYR2*%CP = 66.980, *ZNF462*%CP = 69.204, *GNAQ*%CP = 65.122, *EGR1*%CP = 66.450 and *TRRAP*%CP = 68.803) on progression (Supplementary Table ST2 and Fig. 4). Conversely, a rise in cellular prevalence with progression was also observed for other set of genes. The average%CP of *MAGI3, PCDHA3, COL6A5* and *TUSC3* at baseline were 0, 55.157, 61.372,79.871 and increased to 55.356, 92.269, 91.531 and 86.732% on progression respectively (Supplementary Table ST2 and Fig. 4).

Patterns of clonal evolution in MM

QuantumClone analysis revealed most of the patients had 2 founder clones (51.3%) followed by 3 (26.3%) and 1 (21.1%) while 4 founder clones were rarely observed only in 1.3% of the patients (Fig. 5a). Four different patterns of clonal evolution were identified (Fig. 5). Among them, branching pattern was the most predominant found in 75% patients, followed by Linear in 15.8%, Stable in 5.3% and stable with loss of clone in 3.9% patients.

Further casewise details on clonal heterogeneity, individual patterns of clonal evolution, trajectories of founder clones and subclones identified for each of the 76 patients are shown in Supplementary Fig. 2. This figure shows fish plots, evolution plots as well as the clinical, therapy and demographic details for each patient included in this study. Each subclone had unique cluster of mutations that evolved from baseline to progression, their detailed molecular profiles, cellular prevalence, functional implications and consequences are summarized for each sample in Supplementary Table ST3.

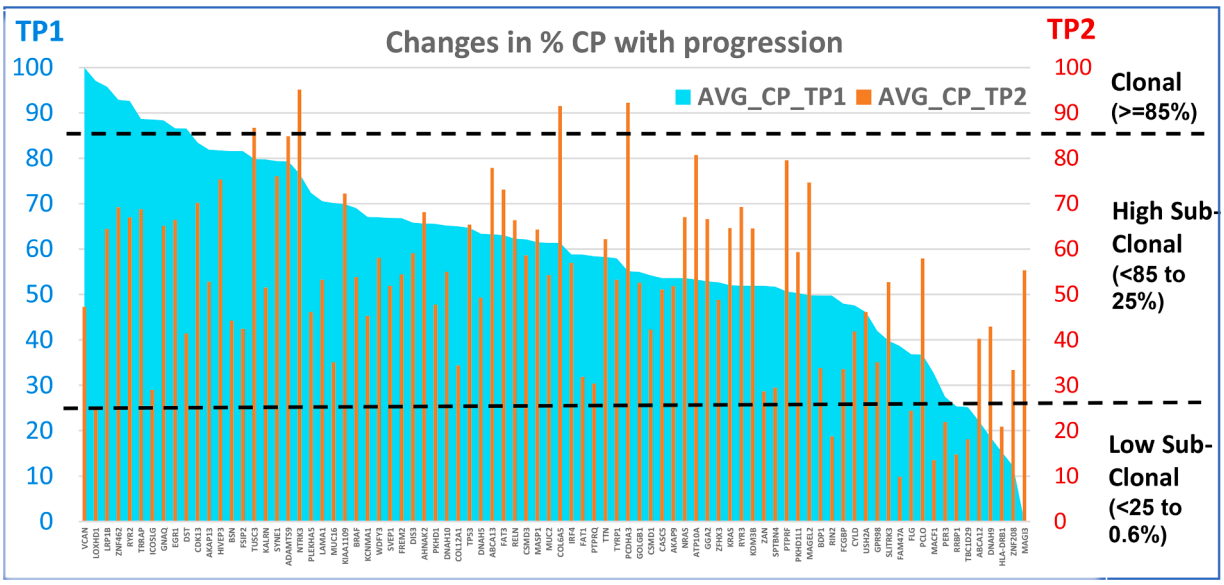

Fig. 4. A comparison of changes in average% Cellular prevalence (%CP) of mutated genes at two time points. Gene mutations were considered as clonal if the%CP was ≥ 85%, high subclonal if between <85 to 25% and low subclonal if between <25 to 0.6%.

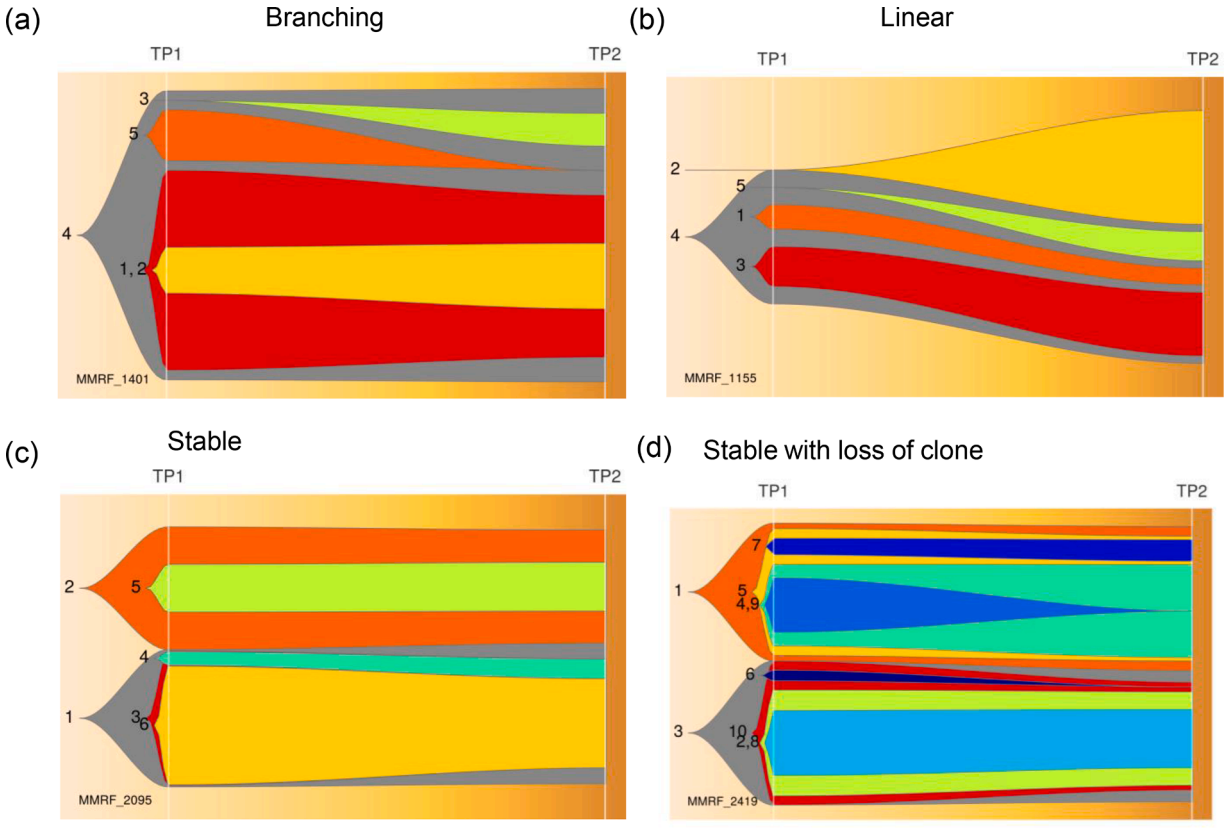

Fig. 5. Four types of clonal evolution patterns observed in MM patients. A representative Fishplot corresponding to each of the four patterns of clonal evolution is shown in (a) Branching, (b) Linear, (c) Stable, and (d) Stable with loss of clone.

Clonal sweeps and correlations of their co-occurrences

Fig. 6 shows a corrgram of individual and concomitant clonal shifts of pairwise mutated genes with disease progression in MM. Strength of Pearsons correlation coefficient r is depicted in lower triangle in Fig. 6 and in Supplementary Table ST4 while the significant p values are shown in upper triangle in Fig. 6 and in Supplementary Table ST5. Trajectories of clonal co-gains were identified in at least 3 patients for *NRAS+MAGI3* genes ($p = 0.023$, $r = 0.283$), *KRAS+TP53* ($p = 0.070$, $r = 0.228$), *TP53+ SYNE1* ($p = 0.003$, $r = 0.365$), while gain of *FCGBP* was observed along with reciprocal loss of *FAT3* ($p = 2.969E-10$, $r = 0.689$). Similar corrplots were also generated for patient subsets grouped on the basis of their cytogenetic aberrations (Fig. 6b–f) including hyperdiploid, del(1)p, 1q21+, del(17)p and t(11;14) respectively. Fig. 7a shows

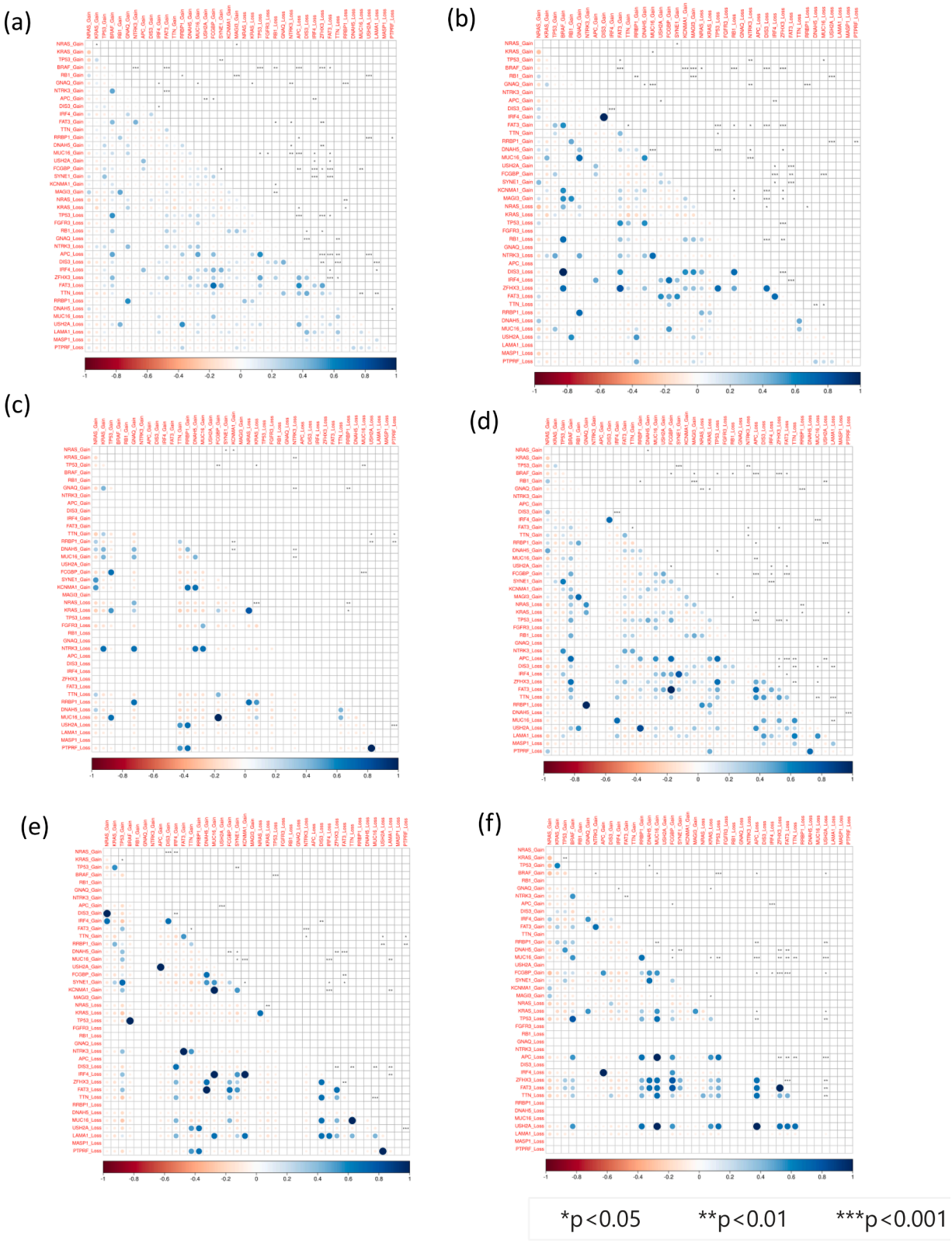

Fig. 6. Corrplot showing pairwise Pearson correlation coefficient r values for co-occurrences of clonal shifts in lower triangle and p values of significance in upper triangle. *$p<0.05$ **$p<0.01$ ***$p<0.001$. Corrplot (a) refers to total patient cohort; (b) patients with Hyperdiploidy (HD); (c) 1p del; (d) 1q gain; (e) 17p del; and (f) samples with t(11;14).

(a)

Cytogenetic Abnormalities	SID	Mutation Co-Gain				
		Same Clone		Different Clone		
HD; del 1p32	MMRF_1030 Δ	TP53+FCGBP+TRRAP		RPS3A		
HD; t(11;14) (CCND1); gain 1q21; del 17p13	MMRF_1137 *	IGLL5+DIS3+IRF4		NRAS		
HD; gain 1q21	MMRF_1153 Δ	FAT3+FOXD4L1		MAGI3	TBC1D29	BRAF
HD; gain 1q21	MMRF_1285 Δ	FCGBP+SYNE1		NRAS		
HD; gain 1q21; del 17p13	MMRF_1533	TP53+FAT3				
t(11;14) (CCND1)	MMRF_1565 Δ	DIS3+FOXD4L1		KRAS	TP53	
HD	MMRF_1880 Δ	NRAS+MAGI3				
HD; gain 1q21	MMRF_2039 *	KMT2B+NFKB2				
CCND2; gain 1q21	MMRF_2059	ACTG1+ZFP36L1	EFTUD2+RASA2			
t(11;14) (CCND1); del 17p13	MMRF_2083 * Δ	KRAS+TP53				
HD; gain 1q21	MMRF_2126 * Δ	NRAS+EGR1				
HD; gain 1q21	MMRF_2330 Δ	NRAS+CR1				
t(4;14) (FGFR3, WHSC1); gain 1q21; del 17p13	MMRF_2531 Δ	SYNE1+KLHL36		TP53	KRAS	ATM
t(11;14) (CCND1); gain 1q21	MMRF_2535 * Δ	FCGBP+BRAF				
t(11;14) (CCND1)	MMRF_1790 * Δ	HUWE1+PRKD2		IRF4	IGLL5	
HD; gain 1q21	MMRF_1639 *	MAGI3+RB1	NRAS+IRAK1	UBR5		
HD; del 1p32	MMRF_1155 Δ	HUWE1+MAX		KRAS		
HD; t(11;14) (CCND1); del 1p32	MMRF_1223	SYNE1+CR1		NRAS		
HD; t(11;14) (CCND1)	MMRF_1352	FCGBP+TRRAP+EP300				
HD	MMRF_1995	NRAS+ACTG1		SYNE1		
HD	MMRF_1293 Δ	KRAS+HIST1H1E	PARP4+USP8			
	MMRF_1424 Δ	TP53+LRP1B				
HD; gain 1q21	MMRF_2344	CYLD+TCL1A	FOXD4L1+PABPC1	HIST1H1E		
t(11;14) (CCND1)	MMRF_1838 Δ	IRF4+TBC1D29		NRAS		
t(11;14) (CCND1); del 17p13	MMRF_1670 Δ	TP53+IGLL5	FCGBP+PRKD2	MAX	SYNE1	
HD; gain 1q21	MMRF_2089 Δ	FAT3+TRRAP+BTG1		NUP214	NRAS	ARHGAP5
t(11;14) (CCND1); gain 1q21	MMRF_1671 Δ	KRAS+FAT3				
HD; t(11;14) (CCND1); gain 1q21	MMRF_1401 * Δ			KMT2B		
HD; t(9;22); t(14;20) (MAFB); del 17p13; del 1p32	MMRF_2076 Δ			FCGBP	IGLL5	
t(11;14) (CCND1)	MMRF_2102 Δ			MAML2	NRAS	
HD; gain 1q21; del 1p32	MMRF_2523 *					
HD	MMRF_2572 Δ					
CCND2; gain 1q21	MMRF_2490			DUSP2	ZFP36L1	
t(4;14) (FGFR3, WHSC1); del 1p32	MMRF_1462			KRAS		

* Progression to death Δ Triplet as 1st treatment

(b)

C (Cyclophosphamide)	CDKN1B, CR1, EGR1, IRF4, NUP214, TP53
Da (Dabrafenib)	BRAF, KRAS, NRAS
K (Carfilzomib)	AR, TP53
P (Pomalidomide)	BRAF
R (Lenalidomide)	BRAF, IRF4, NFKB2, TP53
T (Thalidomide)	BRAF, CCND1, IRF4, NFKBIA, PIM1, SETD2, TP53
Tr (Trametinib)	BRAF, KRAS, NRAS
V (Bortezomib)	AR, ATM, CCND1, CDKN1B, EGR1, IRAK1, IRF4, NFKB2, NFKBIA, PRDM1, PTPN11, RB1, SETD2, TP53, TRRAP, XBP1
d (Dexamethasone)	AR, BTG1, CCND1, CDKN1B, COL1A1, EP300, FAM46C, FGFR3, LTB, NFKB2, NFKBIA, RB1, TP53, ZFP36L1

(c)

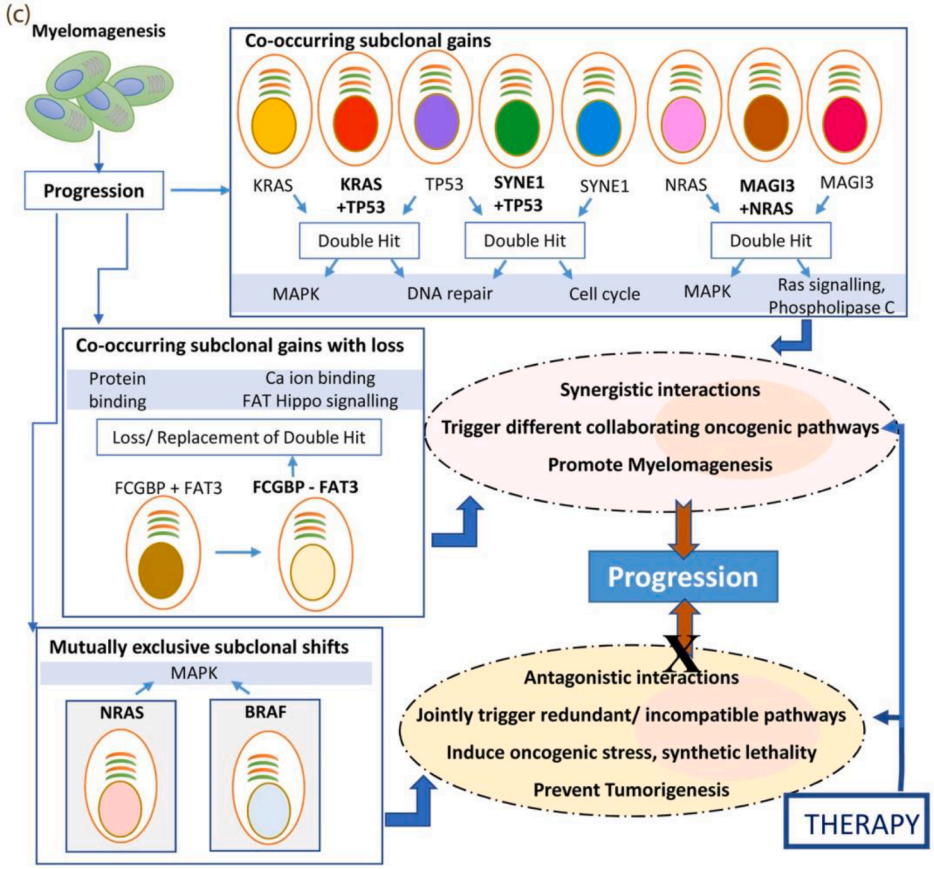

Fig. 7. Molecular profiles of mutational landscapes and 'Double hits' of subclonal shifts observed during progression of myelomatogenesis. (a) Depicts list of co-occurrences of mutations in same clones or in different clones in patients and the cytogenetic abnormalities, (b) Summary of drug pathway genes that may act as target genes or are involved in regulating drug sensitivities, (c) Cartoon showing three types of subclonal shifts (Co-occurring subclonal gains, Co-occurring subclonal gains with loss and mutually exclusive) that can be observed either within same clone or separate clones.. The co-occurring clonal shifts (Co-occurring subclonal gains or Co-occurring subclonal gains with loss) act like 'Double hits' and when present in same clone may promote progression by altering multiple pathways synergistically whereas mutually exclusive clonal shifts tend to result in antagonist synthetic lethal interactions that prevent tumorigenesis. The pathways triggered by such clonal shifts could be explored for development of novel and risk appropriate combinatorial therapies.

subclonal mutational landscapes of MM patients and co-occurring mutations in same or different subclones, their probable impact on drug sensitivities (Fig. 7b) and how the subclonal double hits/ loss of double hits and mutual exclusivities could impact myelomatogenesis (Fig. 7c).

Pathway enrichment analysis at two time points

The KEGG biological pathways predicted by Enrichr to be altered significantly in MM at baseline and on progression are shown in Supplementary Table ST6. The top 10 KEGG pathways significantly enriched at TP1 and TP2 are shown in Supplementary Fig. 3a and c respectively. These included ECM receptor interaction, Focal adhesion, PI3K.Akt signaling, calcium signaling and others.

The KEGG pathways that were uniquely perturbed at baseline included Adherens junction, Hippo signaling pathway, Lysine degradation and ATP-binding cassette (ABC) transporters while those altered at progression exclusively included MAPK signaling, autophagy, cellular senescence, apoptosis, protein digestion and others. Similarly, KEGG pathways that were predicted to be altered throughout baseline to progression included ECM receptor interaction, focal adhesion, Calcium signaling, PI3K-Akt signaling, Gap junction and others (Supplementary Table ST6).

Similarly, the top ten hallmark molecular signatures related to various cellular processes at baseline and progression are shown in Supplementary Table ST6 and Supplementary Fig. 3b and d respectively. The topmost significant MSigs included Epithelial mesenchymal transition, UV response downregulation, Mitotic spindle, Myogenesis and G2-M checkpoint at TP1 while Mitotic Spindle, Myogenesis, Epithelial mesenchymal transition, UV response downregulation, Apical junction, TNF alpha signaling and apoptosis at the time of progression.

Discussion

One of the major reasons for why MM remains undetectable at pre-malignant precursor stages and why it remains incurable is the extent of huge interpatient heterogeneity in genomic composition of malignant plasma cells and their differential abilities to respond to treatment. This highlights the need to identify and better understand clonal evolution of mutational landscapes during myelomatogenesis over time. This would help dissect out drivers and clinically relevant targets of action spanning earliest stages of MGUS/SMM to malignant MM or its relapse.

We have evaluated evolution of clonal mutational signatures with progression in MM. One strength of our study is that we have datamined WES of 76 MM patients that have been sampled at multiple time points in the largest ever genomic study on MM (MMRF CoMMpass). We have used a novel approach of comparing subclonal gains and losses across all the patients (Supplementary Tables ST2, ST3), and for the first time interpreted pairwise correlations of subclonal co-occurrences and exclusions with progression (Fig. 7). For example, in patient MMRF1137, a simultaneous co-gain of mutations in *DIS3* and *IRF4* was observed within the same clone which was also significant in the correlation plot in Fig. 6. This patient ultimately died from disease progression. This study has, therefore, provided a novel insight on how paired driver mutations may preferentially coexist and interact in the same subclones in patients with different cytogenetic aberrations. Their subclonal oncogenic dependencies may have a double hit impact, drive drug resistance and worsen outcomes. Analysis of differential cytogenetic subgroups revealed a few unique significant pairwise correlations (Fig. 6). These correlation profiles included *BRAF*+*FAT3, TP53*+*FAT3, DNAH5*+*GNAQ, BRAF*+*KCNMA1, MUC16*+*RRBP1* among patients with hyperdiploidy; *NRAS*+*DNAH5, RB1*+*FCGBP, USH2A*+*FCGBP* with 1q gain; *TP53*+*FCGBP, NRAS*+*KCNMA1, RRBP1*+*KCNMA1, DNAH5*+*KCNMA1* with 1pdel; *NRAS*+*DIS3, MUC16*+*KCNMA1* with 17pdel; and *BRAF*+*MUC16, RRBP1*+*MUC16, APC*+*FCGBP, FCGBP*+*MUC16* with t (11;14). Further studies will be needed in future to understand the biological and clinical impact of such subclonal correlations in MM.

Our study has revealed three categories of clonal shifts (Fig. 7c). Firstly, co-occurring gains of mutations in drivers such as *KRAS*+*TP53, SYNE1*+*TP53, MAGI3*+*NRAS* that may occur in different clones or within the same clone and result in collaborative oncogenic 'Double Hits'. The second category is represented by co-occurring subclonal gains with gradual loss among *FCGBP*+*FAT3* that may result in loss of 'Double hits' yet oncogenic. The third category includes mutual exclusion of driver genes e.g., *NRAS* and *BRAF* (Fig. 7c). In line with earlier studies [21], subclonal gains of 'double hits' of driver mutations may lead to synergistic interactions across different oncogenic pathways and promote tumorigenesis. Gradual loss of 'Double hits' may also trigger different collaborating oncogenic cascade of events and favor progression. On the contrary, mutual exclusion of other drivers such as *NRAS* and *BRAF* may jointly activate either redundant or incompatible divergent pathways resulting in oncogenic stress, synthetic lethality and prevent tumorigenesis [21]. Mutations in *BRAF, NRAS* and *KRAS* genes are frequently encountered in MM at frequencies of about 20%, 25% and 8% respectively. These are involved in the MAPK pathway [53], regulate proteasome assembly [54], and are potential targets for checkpoint therapy and IMiDs [55]. The mutual exclusion propensities of *NRAS* and *BRAF* are also well established in case of melanoma [56] and our study like others suggests it is operational in MM as well. However, these mutually exclusive genes may tend to co-emerge on treatment with RAF inhibitors. Co-operativity between *KRAS* and *TP53* has been reported in pancreatic cancer [57] and substantiates our findings in the context of MM.

The genes identified to be involved in synergistic or antagonistic interactive clonal 'double hits' leading to progression in MM in this study are key regulatory genes involved in oncogenesis and foster further investigations. Gene *SYNE1* (alias Nesprin1) Spectrin Repeat containing nuclear envelope protein1 is located on chromosome 6q25.2. It links actin cytoskeleton to organelles, maintains nuclear polarity, spindle orientation and subcellular cellular organization. It has a role in nucleotide binding, cell cycle, mitosis, meiosis and DNA damage response. It is known to be somatically mutated or silenced by methylation in breast, prostate, colon, lung cancers, head and neck squamous cell carcinoma suggesting its loss of function may promote tumorigenesis. It has been reported in an isolated case of MM with drug resistance to Bortezomib [58] and needs to be explored further. *MAGI3* gene (alias KIAA1634) (1p13.2) is a membrane associated guanylate kinase that cooperates with *PTEN* to modulate kinase activity of AKT1. It regulates JNK signaling, Ras signaling and phospholipase C pathways. Aberrations in *MAGI3* have been associated with ovarian cancer and *MAGI3-AKT3* fusions occur in breast cancer. It is a known level 3 presumptive evidence based gene implicated in MMSET group of myeloma [59]. *FAT3* (alias KIAA1989) (11q14.3) is a FAT atypical cadherin3 involved in FAT-Hippo signaling and calcium ion binding. It has been associated with TMB and poor prognosis in oesophageal carcinoma. It is found in 4–7% MM patients [60]. The *FCGBP* (Fc fragment of IgG binding protein) (19q13.2) gene has been implicated in melanoma and it forms an integral component of transcriptional networks in MM [61].

In addition to above, we have also analyzed genewise cellular prevalence during clonal shifts and shown presence of trajectories ranging from clonal to subclonal levels for genes such as *LOXHD1* and *ICOSLG* (Fig. 4). Another novel finding of our study is that we have been able to compare the actionable mutational blueprints of subclones at multiple time points in each patient (summarised in Supplementary Table ST3, Supplementary Fig. SF1) that provides a direction to eventually infer personalized genome prescribed combinatorial therapies in future. This study has analyzed association of subclonal mutational gains with probable drug resistance (Fig. 7b). For example, subclonal mutations in *BRAF, IRF4, NFKB2* and *TP53* may affect response to Lenalidomide. Similarly, mutations in *ATM, CCND1, RB1* etc. are involved in Bortezomib response pathway. Hence, regular monitoring of subclonal sweeps of driver mutations at diagnosis and at every relapse may help predict responsiveness to different drugs.

Parallel studies carried out on clonal evolution of MM by others also lend support to predominance of branching evolution [30,35,62] as observed in our analysis. A similar analysis of sequential WES of 10 patients from MGUS to MM highlighted that the transformed subclonal PC populations identified at MM are already present in asymptomatic MGUS/SMM stages and are thus reflective of clonal stability [36]. Another study [38] on WES of 19 patients enrolled in MMRF CoMMpass genomic project study showed that stable/resistant clones were characterized by concurrent 17pdel and 13qdel, and/or mutations in *NRAS, DIS3, FAM46C, ROBO1* and *CCND1*. A longitudinal follow-up of clonal trajectories from early initiation or time of diagnosis to malignant transformation / relapse may therefore allow identification of subclones that are stable/resistant or sensitive to line of treatment [36].

A recent study [37] has further proposed that alternate punctuated episodes of emergence of new subclones driven to dominance followed by their static expansion under positive selection continue across multiple time windows of myelomatogenesis. This process during early initiation prior to SMM leads to preservation of a clonal architecture with malignant potential that might expand and evolve further until clinical significance. It has been suggested that retention of a parallel architecture in MM as of SMM could be probed for better prognostication and early intervention [37].

Conclusions

The differences in oncogenic genes and associated pathway networks at two time points of evaluation reflect a continuum of clonal evolution that may be explored as an additional independent mechanism of drug resistance observed in clinical practice. Besides, these findings are important conceptually as they highlight the need for (1) molecular testing immediately before initiating a new therapy especially if aiming at a targeted or immune therapy, (2) estimation of cellular prevalence to predict the likelihood of the depth of response achievable with targeted therapy and rationalized approach on combining multiple therapeutics and (3) single cell mutation spectrum profiling at least for patients under evaluation in clinical trials with novel therapeutics and to explore the relevance of subclonal double hits.

Data availability

The IA12 datasets used for the analyses described in this work were downloaded from MMRF CoMMpass (Multiple Myeloma Research Foundation CoMMpass [SM] (Relating Clinical Outcomes in MM to Personal Assessment of Genetic Profile) study (www.themmrf.org)) researcher gateway.

Author contributions

RG conceived and designed the study, contributed in clinical analysis, data interpretation and wrote the manuscript. GK, LJ, AF and SK performed analysis, data interpretations and wrote the manuscript. AG coordinated computational analysis and wrote the manuscript.

Ethical information statement

This is a computational study that has analyzed publicly available online datasets generated by the Multiple Myeloma Research Foundation (MMRF) Personalized Medicine Initiatives (https://research.themmrf.org and www.themmrf.org). These data were downloaded directly from MMRF researcher gateway with due permission granted by the MMRF. Since no samples were collected from human/animal subjects in this study, ethical approval and informed consents are not applicable.

Conflicts of interest

The authors declare that there is no conflict of interests of any kind regarding the publication of this paper.

Acknowledgements

This work was supported by grants from Department of Biotechnology, Govt. of India [BT/ PR7136 /MED /30/901/2012; BT/MED/30/SP11006/2015] and Department of Science and Technology, Govt. of India [DST/ICPS/CPS-Individual/2018/279(G)]. Akanksha Farswan would like to thank University Grants Commission, Govt. of India for UGC-Senior Research Fellowship. Authors acknowledge Multiple Myeloma Research Foundation (MMRF) for providing the CoMMpass IA12 dataset. These data were generated as part of the Multiple Myeloma Research Foundation Personalized Medicine Initiatives (https://research.themmrf.org and www.themmrf.org). Dr. Anubha Gupta would also like to thank Infosys Center for Artificial Intelligence, IIIT-Delhi for support in their research.

Supplementary materials

Supplementary material associated with this article can be found, in the online version, at doi:10.1016/j.tranon.2022.101472.

References

[1] NWCJ van de Donk, C. Pawlyn, K.L Yong, Multiple myeloma. The Lancet, Elsevier 397 (2021) 410–427, https://doi.org/10.1016/S0140-6736(21)00135-5.
[2] B.A. Walker, C.P. Wardell, L. Melchor, A. Brioli, D.C. Johnson, M.F. Kaiser, Intraclonal heterogeneity is a critical early event in the development of myeloma and precedes the development of clinical symptoms, Leukemia 28 (2014) 384–390, https://doi.org/10.1038/leu.2013.199.
[3] S.V. Rajkumar, Updated diagnostic criteria and staging system for multiple myeloma, Am. Soc. Clin. Oncol. Educ. Book Am. Soc. Clin. Oncol. Meet. 35 (2016) e418–e423, https://doi.org/10.14694/EDBK_159009.
[4] S. Manier, K.Z. Salem, J. Park, D.A. Landau, G. Getz, I.M. Ghobrial, Genomic complexity of multiple myeloma and its clinical implications, Nat. Rev. Clin. Oncol. 14 (2016) 100–113, https://doi.org/10.1038/nrclinonc.2016.122.
[5] S.K. Kumar, S.V. Rajkumar, The multiple myelomas — Current concepts in cytogenetic classification and therapy, in: Nat Rev Clin Oncol, 15, Nature Publishing Group, 2018, pp. 409–421, https://doi.org/10.1038/s41571-018-0018-y.
[6] O. Landgren, G.J. Morgan, Biologic frontiers in multiple myeloma: from biomarker identification to clinical practice, Clin Cancer Res. Am. Assoc. Cancer Res. 20 (2014) 804–813, https://doi.org/10.1158/1078-0432.CCR-13-2159.
[7] H. Kaufmann, J. Ackermann, C. Baldia, T. Nösslinger, R. Wieser, S. Seidl, V. Sagaster, H. Gisslinger, U. Jäger, M. Pfeilstöcker, C. Zielinski, J. Drach, Both IGH translocations and chromosome 13q deletions are early events in monoclonal gammopathy of undetermined significance and do not evolve during transition to multiple myeloma, Leukemia 18 (2004) 1879–1882, https://doi.org/10.1038/sj.leu.2403518.
[8] H. Avet-Loiseau, C. Li, F. Magrangeas, W. Gouraud, C. Charbonnel, J.-. L. Harousseau, M. Attal, G. Marit, C. Mathiot, T. Facon, P. Moreau, K.C. Anderson, L. Campion, et al., Prognostic significance of copy-number alterations in multiple myeloma, J. Clin. Oncol. Off. J. Am. Soc. Clin. Oncol. 27 (2009) 4585–4590, https://doi.org/10.1200/JCO.2008.20.6136.
[9] D.R. Carrasco, G. Tonon, Y. Huang, Y. Zhang, R. Sinha, B. Feng, J.P. Stewart, F. Zhan, D. Khatry, M. Protopopova, A. Protopopov, K. Sukhdeo, I. Hanamura, et al., High-resolution genomic profiles define distinct clinico-pathogenetic subgroups of multiple myeloma patients, Cancer Cell 9 (2006) 313–325, https://doi.org/10.1016/j.ccr.2006.03.019.
[10] N. Abdallah, S.V. Rajkumar, P. Greipp, P. Kapoor, M.A. Gertz, A. Dispenzieri, L. B. Baughn, M.Q. Lacy, S.R. Hayman, F.K. Buadi, D. Dingli, R.S. Go, Y.L. Hwa, et al., Cytogenetic abnormalities in multiple myeloma: association with disease characteristics and treatment response, Blood Cancer J. 10 (2020) 82, https://doi.org/10.1038/s41408-020-00348-5.
[11] CoMMpass Network TM A. Christofferson, S. Skerget, J. Aldrich, C. Legendre, S. Nasser, J. Yesil, D. Auclair, S. Lonial, J.J Keats, Unsupervised Clustering of DNA Copy Number Profiles Identifies a High-Risk Subtype of Hyperdiploid Multiple Myeloma: an Mmrf Commpass Analysis, Blood. Am. Soc. Hematol. 134 (2019), https://doi.org/10.1182/blood-2019-132152, 1805–1805.
[12] S. Skerget, A. Christofferson, S. Nasser, C. Legendre, J. Yesil, D. Auclair, S. Lonial, J. Keats, Identification and Molecular Characterization of High-Risk Multiple Myeloma Patients from the MMRF CoMMpass Study at Diagnosis and Progression, in: Clin Lymphoma Myeloma Leuk, 19, Elsevier, 2019, p. e7, https://doi.org/10.1016/j.clml.2019.09.009.

[13] Skerget S., Penaherrera D., Chari A., Jagannath S., Siegel D.S., Vij R., Orloff G., Jakubowiak A., Niesvizky R., Liles D., Berdeja J., Levy M., Wolf J., et al. Genomic Basis of Multiple Myeloma Subtypes from the MMRF CoMMpass Study [Internet]. 2021 Aug p. 2021.08.02.21261211. Available from https://www.medrxiv.org/content/10.1101/2021.08.02.21261211v1.

[14] O. Castaneda, R. Baz, Multiple Myeloma Genomics - A Concise Review, Acta Medica Acad. 48 (2019) 57–67, https://doi.org/10.5644/ama2006-124.242.

[15] J.R. Sawyer, The prognostic significance of cytogenetics and molecular profiling in multiple myeloma, Cancer Genet. 204 (2011) 3–12, https://doi.org/10.1016/j.cancergencyto.2010.11.002.

[16] N.C. Munshi, H. Avet-Loiseau, Genomics in multiple myeloma, Clin. Cancer Res. Off. J. Am. Assoc. Cancer Res. 17 (2011) 1234–1242, https://doi.org/10.1158/1078-0432.CCR-10-1843.

[17] S. Robiou du Pont, A. Cleynen, C. Fontan, M. Attal, N. Munshi, J. Corre, H. Avet-Loiseau, Genomics of Multiple Myeloma, J. Clin. Oncol. 35 (2017) 963–967, https://doi.org/10.1200/jco.2016.70.6705.

[18] N. Bolli, G. Biancon, M. Moarii, S. Gimondi, Y. Li, C. de Philippis, F. Maura, V. Sathiaseelan, Y.-.T. Tai, L. Mudie, S. O'Meara, K. Raine, J.W. Teague, et al., Analysis of the genomic landscape of multiple myeloma highlights novel prognostic markers and disease subgroups, Leukemia (2017), https://doi.org/10.1038/leu.2017.344.

[19] M. Hultcrantz, Genomic Landscape and Mechanisms of Disease Evolution and Progression in Multiple Myeloma, Am. J. Hematol. Oncol. (2017) [Internet][cited 2021 Aug 30]; 13. Available from, https://www.gotoper.com/publications/ajho/2017/2017december/genomic-landscape-and-mechanisms-of-disease-evolution-and-progression-in-multiple-myeloma.

[20] A. Laganà, D. Perumal, D. Melnekoff, B. Readhead, B.A. Kidd, V. Leshchenko, P.-.Y. Kuo, J. Keats, M. DeRome, J. Yesil, D. Auclair, S. Lonial, A. Chari, et al., Integrative network analysis identifies novel drivers of pathogenesis and progression in newly diagnosed multiple myeloma, Leukemia 32 (2018) 120–130, https://doi.org/10.1038/leu.2017.197.

[21] G. El Tekle, T. Bernasocchi, A.M. Unni, F. Bertoni, D. Rossi, M.A. Rubin, J.-.P. Theurillat, Co-occurrence and mutual exclusivity: what cross-cancer mutation patterns can tell us, Trends Cancer 7 (2021) 823–836, https://doi.org/10.1016/j.trecan.2021.04.009.

[22] B.A. Walker, K. Mavrommatis, C.P. Wardell, T.C. Ashby, M. Bauer, F.E. Davies, A. Rosenthal, H. Wang, P. Qu, A. Hoering, M. Samur, F. Towfic, M. Ortiz, et al., Identification of novel mutational drivers reveals oncogene dependencies in multiple myeloma, Blood 132 (2018) 587–597, https://doi.org/10.1182/blood-2018-03-840132.

[23] F. Maura, E.M. Boyle, E.H. Rustad, C. Ashby, D. Kaminetzky, B. Bruno, M. Braunstein, M. Bauer, P. Blaney, Y. Wang, H. Ghamlouch, L. Williams, J. Stoeckle, et al., Chromothripsis as a pathogenic driver of multiple myeloma, Semin. Cell Dev. Biol. (2021), https://doi.org/10.1016/j.semcdb.2021.04.014 [Internet][cited 2021 Aug 30];.

[24] G. Kaur, R. Gupta, N. Mathur, L. Rani, L. Kumar, A. Sharma, V. Singh, A. Gupta, O. D Sharma, Clinical impact of chromothriptic complex chromosomal rearrangements in newly diagnosed multiple myeloma, Leuk. Res. 76 (2019) 58–64, https://doi.org/10.1016/j.leukres.2018.12.005.

[25] T. Perini, M. Materozzi, E. Milan, The Immunity-malignancy equilibrium in multiple myeloma: lessons from oncogenic events in plasma cells, FEBS J. [Internet] (2021), https://doi.org/10.1111/febs.16068 [citedAug 30]; n/a.

[26] R. Liu, Q. Gao, S.M. Foltz, J.S. Fowles, L. Yao, J.T. Wang, S. Cao, H. Sun, M. C. Wendl, S. Sethuraman, A. Weerasinghe, M.P. Rettig, E.P. Storrs, et al., Co-evolution of tumor and immune cells during progression of multiple myeloma, Nat. Commun. 12 (2021) 2559, https://doi.org/10.1038/s41467-021-22804-x.

[27] P.H. Hoang, R.S. Houlston, Multiple mechanisms can disrupt oncogenic pathways in multiple myeloma, Oncotarget 9 (2018) 35801–35802, https://doi.org/10.18632/oncotarget.26301.

[28] E.M. Boyle, S. Deshpande, R. Tytarenko, C. Ashby, Y. Wang, M.A. Bauer, S. K. Johnson, C.P. Wardell, S. Thanendrarajan, M. Zangari, T. Facon, C. Dumontet, B. Barlogie, et al., The molecular make up of smoldering myeloma highlights the evolutionary pathways leading to multiple myeloma, Nat. Commun. 12 (2021), https://doi.org/10.1038/s41467-020-20524-2 [Internet]. 2021 [citedJun 10].

[29] L. John, M.T. Krauth, K. Podar, M.-.S. Raab, Pathway-Directed Therapy in Multiple Myeloma, Cancers. Multidisciplinary Digital Publishing Institute; 13 (2021) 1668, https://doi.org/10.3390/cancers13071668.

[30] N. Bolli, H. Avet-Loiseau, D.C. Wedge, P. Van Loo, L.B. Alexandrov, I. Martincorena, K.J. Dawson, F. Iorio, S. Nik-Zainal, G.R. Bignell, J.W. Hinton, Y. Li, J.M.C. Tubio, et al., Heterogeneity of genomic evolution and mutational profiles in multiple myeloma, Nat. Commun. 5 (2014) 2997, https://doi.org/10.1038/ncomms3997.

[31] J.G. Lohr, P. Stojanov, S.L. Carter, P. Cruz-Gordillo, M.S. Lawrence, D. Auclair, C. Sougnez, B. Knoechel, J. Gould, G. Saksena, K. Cibulskis, A. McKenna, M. A. Chapman, et al., Widespread genetic heterogeneity in multiple myeloma: implications for targeted therapy, Cancer Cell 25 (2014) 91–101, https://doi.org/10.1016/j.ccr.2013.12.015.

[32] B.A. Walker, E.M. Boyle, C.P. Wardell, A. Murison, D.B. Begum, N.M. Dahir, P. Z. Proszek, D.C. Johnson, M.F. Kaiser, L. Melchor, L.I. Aronson, M. Scales, C. Pawlyn, et al., Mutational spectrum, copy number changes, and outcome: results of a sequencing study of patients with newly diagnosed myeloma, J. Clin. Oncol. Off. J. Am. Soc. Clin. Oncol. 33 (2015) 3911–3920, https://doi.org/10.1200/JCO.2014.59.1503.

[33] M.C. Da Vià, B. Ziccheddu, A. Maeda, F. Bagnoli, G. Perrone, N. Bolli, A Journey Through Myeloma Evolution: from the Normal Plasma Cell to Disease Complexity, HemaSphere 4 (2020) e502, https://doi.org/10.1097/HS9.0000000000000502.

[34] M. Ho, A. Patel, C.Y. Goh, M. Moscvin, L. Zhang, G. Bianchi, Changing paradigms in diagnosis and treatment of monoclonal gammopathy of undetermined significance (MGUS) and smoldering multiple myeloma (SMM), Leukemia 34 (2020) 3111–3125, https://doi.org/10.1038/s41375-020-01051-x.

[35] N. Bolli, F. Maura, S. Minvielle, D. Gloznik, R. Szalat, A. Fullam, I. Martincorena, K. J. Dawson, M.K. Samur, J. Zamora, P. Tarpey, H. Davies, M. Fulciniti, et al., Genomic patterns of progression in smoldering multiple myeloma, Nat. Commun. 9 (2018) 3363, https://doi.org/10.1038/s41467-018-05058-y.

[36] A.K. Dutta, J.L. Fink, J.P. Grady, G.J. Morgan, C.G. Mullighan, L.B. To, D. R. Hewett, A.C.W. Zannettino, Subclonal evolution in disease progression from MGUS/SMM to multiple myeloma is characterised by clonal stability, Leukemia 33 (2019) 457–468, https://doi.org/10.1038/s41375-018-0206-x.

[37] B. Diamond, V. Yellapantula, E.H. Rustad, K.H. Maclachlan, M. Mayerhoefer, M. Kaiser, G. Morgan, O. Landgren, F. Maura, Positive selection as the unifying force for clonal evolution in multiple myeloma, Leukemia 35 (2021) 1511–1515, https://doi.org/10.1038/s41375-021-01130-7.

[38] A. Lagana, D. Melnekoff, I. Beno, V. Leshchenko, D. Perumal, J.J. Keats, M. DeRome, J. Yesil, D. Auclair, D. Madduri, A. Chari, H.J. Cho, B. Barlogie, et al., Clonal Evolution in Newly Diagnosed Multiple Myeloma Patients: a Follow-up Study from the Mmrf Commpass Genomics Project, Blood 130 (2017) 325, https://doi.org/10.1182/blood.V130.Suppl_1.325.325.

[39] F. Maura, E.H. Rustad, E.M. Boyle, G.J. Morgan, Reconstructing the evolutionary history of multiple myeloma, Best Pract. Res. Clin. Haematol. 33 (2020), 101145, https://doi.org/10.1016/j.beha.2020.101145.

[40] E. Talevich, A.H. Shain, T. Botton, Bastian BC. CNVkit, Genome-Wide Copy Number Detection and Visualization from Targeted DNA Sequencing, PLoS Comput. Biol. 12 (2016), e1004873, https://doi.org/10.1371/journal.pcbi.1004873.

[41] P. Deveau, L. Colmet Daage, D. Oldridge, V. Bernard, A. Bellini, M. Chicard, N. Clement, E. Lapouble, V. Combaret, A. Boland, V. Meyer, J.-.F. Deleuze, I. Janoueix-Lerosey, et al., QuantumClone: clonal assessment of functional mutations in cancer based on a genotype-aware method for clonal reconstruction, Bioinformatics. Oxford Acad. 34 (2018) 1808–1816, https://doi.org/10.1093/bioinformatics/bty016.

[42] M. Ca, M. J, D. Hx, M. Ca, D. L, L. Tj, M. Er, W Rk, Visualizing tumor evolution with the fishplot package for R, BMC Genomics [Internet]. BMC Genom. 17 (2016), https://doi.org/10.1186/s12864-016-3195-z [cited 2021 Aug 25].

[43] W. Jiao, S. Vembu, A.G. Deshwar, L. Stein, Q. Morris, Inferring clonal evolution of tumors from single nucleotide somatic mutations, BMC Bioinformatics 15 (2014) 35, https://doi.org/10.1186/1471-2105-15-35.

[44] X. Ma, M. Edmonson, D. Yergeau, D.M. Muzny, O.A. Hampton, M. Rusch, G. Song, J. Easton, R.C. Harvey, D.A. Wheeler, J. Ma, H. Doddapaneni, B. Vadodaria, et al., Rise and fall of subclones from diagnosis to relapse in pediatric B-acute lymphoblastic leukaemia, Nat. Commun. 6 (2015) 6604, https://doi.org/10.1038/ncomms7604.

[45] J.R. Jones, N. Weinhold, C. Ashby, B.A. Walker, C. Wardell, C. Pawlyn, L. Rasche, L. Melchor, D.A. Cairns, W.M. Gregory, D. Johnson, D.B. Begum, S. Ellis, et al., Clonal evolution in myeloma: the impact of maintenance lenalidomide and depth of response on the genetics and sub-clonal structure of relapsed disease in uniformly treated newly diagnosed patients, Haematologica 104 (2019) 1440–1450, https://doi.org/10.3324/haematol.2018.202200.

[46] F. Nadeu, G. Clot, J. Delgado, D. Martín-García, T. Baumann, I. Salaverria, S. Beà, M. Pinyol, P. Jares, A. Navarro, H. Suárez-Cisneros, M. Aymerich, M. Rozman, et al., Clinical impact of the subclonal architecture and mutational complexity in chronic lymphocytic leukemia, Leukemia 32 (2018) 645–653, https://doi.org/10.1038/leu.2017.291.

[47] A. Gonzalez-Perez, C. Perez-Llamas, J. Deu-Pons, D. Tamborero, M.P. Schroeder, A. Jene-Sanz, A. Santos, N Lopez-Bigas, IntOGen-mutations identifies cancer drivers across tumor types, Nat. Methods 10 (2013) 1081–1082, https://doi.org/10.1038/nmeth.2642.

[48] D. Chakravarty, J. Gao, S.M. Phillips, R. Kundra, H. Zhang, J. Wang, J.E. Rudolph, R. Yaeger, T. Soumerai, M.H. Nissan, M.T. Chang, S. Chandarlapaty, T.A. Traina, et al., OncoKB: a precision oncology knowledge base, JCO Precis. Oncol. (2017), https://doi.org/10.1200/PO.17.00011, 2017PO.17.00011.

[49] J. Gao, B.A. Aksoy, U. Dogrusoz, G. Dresdner, B. Gross, S.O. Sumer, Y. Sun, A. Jacobsen, R. Sinha, E. Larsson, E. Cerami, C. Sander, N. Schultz, Integrative analysis of complex cancer genomics and clinical profiles using the cBioPortal, Sci. Signal. 6 (2013) pl1, https://doi.org/10.1126/scisignal.2004088.

[50] E. Cerami, J. Gao, U. Dogrusoz, B.E. Gross, S.O. Sumer, B.A. Aksoy, A. Jacobsen, C. J. Byrne, M.L. Heuer, E. Larsson, Y. Antipin, B. Reva, A.P. Goldberg, et al., The cBio cancer genomics portal: an open platform for exploring multidimensional cancer genomics data, Cancer Discov. 2 (2012) 401–404, https://doi.org/10.1158/2159-8290.CD-12-0095.

[51] M.V. Kuleshov, M.R. Jones, A.D. Rouillard, N.F. Fernandez, Q. Duan, Z. Wang, S. Koplev, S.L. Jenkins, K.M. Jagodnik, A. Lachmann, M.G. McDermott, C. D. Monteiro, G.W. Gundersen, et al., Enrichr: a comprehensive gene set enrichment analysis web server 2016 update, Nucleic Acids Res. 44 (2016) W90–W97, https://doi.org/10.1093/nar/gkw377.

[52] A. Liberzon, C. Birger, H. Thorvaldsdóttir, M. Ghandi, J.P. Mesirov, P. Tamayo, The Molecular Signatures Database (MSigDB) hallmark gene set collection, Cell Syst. 1 (2015) 417–425, https://doi.org/10.1016/j.cels.2015.12.004.

[53] M. Lionetti, M. Barbieri, K. Todoerti, L. Agnelli, S. Marzorati, S. Fabris, G. Ciceri, S. Galletti, G. Milesi, M. Manzoni, M. Mazzoni, A. Greco, G. Tonon, et al., Molecular spectrum of BRAF, NRAS and KRAS gene mutations in plasma cell dyscrasias: implication for MEK-ERK pathway activation, Oncotarget. Impact J. 6 (2015) 24205–24217, https://doi.org/10.18632/oncotarget.4434.

[54] F. Shirazi, R.J. Jones, R.K. Singh, J. Zou, I. Kuiatse, Z. Berkova, H. Wang, H.C. Lee, S. Hong, L. Dick, N. Chattopadhyay, R.Z. Orlowski, Activating KRAS, NRAS, and BRAF mutants enhance proteasome capacity and reduce endoplasmic reticulum stress in multiple myeloma, Proc. Natl. Acad. Sci. Proc. Natl. Acad. Sci. 117 (2020) 20004–20014, https://doi.org/10.1073/pnas.2005052117.

[55] S. Pasca, C. Tomuleasa, P. Teodorescu, G. Ghiaur, D. Dima, V. Moisoiu, C. Berce, C. Stefan, A. Ciechanover, H Einsele, KRAS/NRAS/BRAF mutations as potential targets in multiple myeloma, Front. Oncol. 9 (2019) 1137, https://doi.org/10.3389/fonc.2019.01137.

[56] C. Petti, A. Molla, C. Vegetti, S. Ferrone, A. Anichini, M. Sensi, Coexpression of NRASQ61R and BRAFV600E in human melanoma cells activates senescence and increases susceptibility to cell-mediated cytotoxicity, Cancer Res. 66 (2006) 6503–6511, https://doi.org/10.1158/0008-5472.CAN-05-4671.

[57] M.P. Kim, X. Li, J. Deng, Y. Zhang, B. Dai, K.L. Allton, T.G. Hughes, C. Siangco, J. J. Augustine, Y. Kang, J.M. McDaniel, S. Xiong, E.J. Koay, et al., Oncogenic KRAS recruits an expansive transcriptional network through mutant p53 to drive pancreatic cancer metastasis, Cancer Discov. Am. Assoc. Cancer Res. 11 (2021) 2094–2111, https://doi.org/10.1158/2159-8290.CD-20-1228.

[58] H. Ikeda, K. Ishiguro, Y. Aoki, T. Igarashi, T. Hayashi, T. Ishida, Y. Sasaki, T. Tokino, Y. Shinomura, Molecular diagnostics of a single drug-resistant multiple myeloma case using targeted next-generation sequencing, OncoTargets Ther. (2015) 2805, https://doi.org/10.2147/ott.s86515.

[59] Alberge J.-.B., Magrangeas F., Wagner M., Denié S., Guérin-Charbonnel C., Campion L., Attal M., Avet-Loiseau H., Carell T., Moreau P., Minvielle S., Sérandour A.A. DNA hydroxymethylation reveals transcription regulation networks and prognostic signatures in multiple myeloma [Internet]. 2019 Oct p. 806133. Available from https://www.biorxiv.org/content/10.1101/806133v1.

[60] I.J. Cardona-Benavides, C. de Ramón, N.C. Gutiérrez, Genetic abnormalities in multiple myeloma: prognostic and therapeutic implications, Cells 10 (2021) 336, https://doi.org/10.3390/cells10020336.

[61] L. Agnelli, M. Forcato, F. Ferrari, G. Tuana, K. Todoerti, B.A. Walker, G.J. Morgan, L. Lombardi, S. Bicciato, A. Neri, The reconstruction of transcriptional networks reveals critical genes with implications for clinical outcome of multiple myeloma, Clin Cancer Res. Am. Assoc. Cancer Res. 17 (2011) 7402–7412, https://doi.org/10.1158/1078-0432.CCR-11-0596.

[62] Y. Furukawa, J. Kikuchi, Molecular pathogenesis of multiple myeloma, Int. J. Clin. Oncol. 20 (2015) 413–422, https://doi.org/10.1007/s10147-015-0837-0.